Conf-790302--18

UCRL-13967

COOLDOWN AND WARMUP THERMAL ANALYSIS OF THE MIRROR FUSION TEST FACILITY (MFTF) SUPERCONDUCTING MAGNET

R. F. O'Neill
R. E. Tatro

March 1, 1979

This paper was prepared for submission to the 5th International Conference on Structural Mechanics in Reactor Technology in Berlin, Germany, August 13-17, 1979.

P. O. 9815603

MASTER

GENERAL DYNAMICS

SAN DIEGO, CALIFORNIA

COOLDOWN AND WARMUP THERMAL ANALYSIS OF THE MIRROR FUSION TEST FACILITY (MFTF) SUPERCONDUCTING MAGNET

Authors
Richard F. O'Neill
Robert E. Tatro
General Dynamics Convair Division

SUMMARY

General Dynamics Convair Division has performed a series of detailed cooldown and warmup thermal analyses to support the design of the Lawrence Livermore Laboratory (LLL), Mirror Fusion Test Facility (MFTF) magnet system. The analyses were conducted under LLL Contract 9815603. All analysis objectives were achieved, including definition of a cooldown and warmup operating schedule which can 1) effect complete cooldown and warmup within three to five days (an LLL requirement), 2) yield acceptable levels of thermally-induced stresses resulting from transverse and longitudinal structural temperature differentials, and 3) yield acceptable stress levels with or without flow imbalances in separate sections of the magnet. The analyses were executed through the National Magnetic Fusion Energy Computer Center (MFECC) at LLL.

Cooldown and warmup studies were initiated with the formulation of a detailed, multi-node analysis model of the magnet assuming vertical alignment of the magnet Z-axis. The analysis model conveniently exploited thermal symmetry, in that helium entry and exit locations were always at the major and/or minor radii of each magnet. The model permitted thermal simulation of any section of the total assembly by simple redirection of the helium through-flow nodal arrangement.

Reorientation of the MFTF fusion chamber from the vertical to the horizontal position necessitated an interim redesign of the analysis model. The interim model consisted of two sections containing 629 nodes and 1,280 nodes, respectively. It included simulations of the external case stiffeners and the intercoil structure, and realistically modeled the thermal asymmetry resulting from repositioning of the helium entry and exit locations to the lowest and highest points on each magnet.

Additional case stiffener modifications were simulated in a final version of the cooldown and warmup model. The model was resolved into an arrangement in which regions identified as "Large Model 1" and "Large Model 2" comprised the 1,280-node section of the interim model. In order to provide temperature boundary conditions for the large analysis models, and to permit multiple analyses yielding total system cooldown time, the exacting multi-node simulations in each section of the large models were condensed and assembled into a 44-node small model representing the entire magnet. The small macro-model was then employed in a series of cooldown analyses with flow rates from 51 g/s to 340 g/s.

Large model transverse temperature differentials resulted in acceptable stress levels for flow rates approaching 180 g/s, with a total cooldown time of only 30 hr. However, longitudinal temperature differentials obtained with the small model established the limiting thermal stress levels. Temperature distributions corresponding to the 119 g/s flow rate and the 85 g/s flow rate were imposed on separate legs of a single magnet, and yielded acceptable stress levels. A nominal total flow rate of 100 g/s was recommended, for which the predicted cooldown duration is 82 ± 10 hr.

The MFTF magnet cooldown and warmup thermal analysis models were geometrically similar to, and complemented, the corresponding structural analysis models. These studies have demonstrated the importance of relatively complex thermal-analytical modeling to achieve the necessary definition of transient temperature distributions in large magnet structures.

1. INTRODUCTION

The Lawrence Livermore Laboratory (LLL) Mirror Fusion Test Facility (MFTF), scheduled for completion in July 1981, has the physics goals of 1) investigating the behavior of known instabilities in plasmas approaching the dimensions of a mirror fusion reactor, and 2) attempted confirmation of the plasma scaling laws up to $n\tau = 10^{12}$ cm^{-3}• s. The MFTF has the largest (approximately 318,000 kg) superconducting magnet in the world. The yin-yang pair has an average major radius of 2.5 m, spaced to give a length between plasma mirrors of 3.6 m and a mirror ratio of 2:1. The central field is 2T, corresponding to a peak field of 7.68T at the superconductor. The magnet is suspended in a horizontal, cylindrically configured vacuum vessel capable of sustaining a base pressure of 10^{-8} Torr.

Cooldown of the magnet to its operating temperature of 4.5K is achieved by cryogenic helium through-flow, and a similar flow of warm helium is employed for warmup of the magnet. The General Dynamics Convair Division performed detailed thermal analyses of the cooldown and warmup processes to: 1) assess the sensitivity of cooldown and warmup duration to helium flow rate and supply temperature schedule, 2) support definition of refrigeration requirements in terms of recommended helium flow rates and supply temperatures, and resultant return helium temperatures, and 3) provide detailed definition of structural temperature distributions sustained during the cooldown and warmup transients.

The latter objective is of interest in this paper. It will be seen that the magnet thermal analysis model complements the structural analysis model in terms of node spatial distribution, permitting direct employment of the thermal analysis output data as structural analysis input. This motive was a major determinant of thermal model node density, as were the geometric and thermodynamic complexities of the magnet.

2. THE MFTF MAGNET CONFIGURATION

The magnet is shown in perspective in Figure 1, where the yin-yang assembly is pictured prior to installation of form-fitted LN_2 shielding which enshrouds the entire structure, and local H_2O shields which intercept neutral beam impingement and plasma heat flux. The LN_2 and H_2O shields do not significantly influence magnet cooldown. A typical section of the assembled magnet is shown in Figure 2. The conductor windings are enclosed in a 316 stainless steel jacket, and separated from the jacket by G-11 epoxy insulation on all four sides. The 304 LN stainless steel case is the major structural component of the magnet. Its basic wall thickness is 7.62 cm, except for 12.7-cm inboard sections near the minor radius of each coil. Following weld closure of the jacket and case, the jacket is rigidly potted in place, as shown in Figure 2. Potting material is injected between the jacket and a 260 brass shim bladder, forcing it against the case surfaces. The latter contact is limited to 0.95-cm deep, 5.0-cm diameter dimples which comprise one-half of the total interior surface of the case. Void regions between the dimples serve a dual function: they accommodate helium through-flow for cooldown and warmup of the structure, and they comprise a portion of the separately pumped guard vacuum. The remaining portion of the guard vacuum is provided with interior flow baffles which do not impede post-cooldown pumping of the guard vacuum. However, like the brass shim bladder, they facilitate efficient convective scrubbing of the case by the flowing helium.

Placement of the external case stiffeners is shown in Figures 1 and 2. As shown in Figure 1, the yin-yang pair is separated by intercoil structure at four locations, connecting the major radii of each coil to the opposing coil minor radius coil extension structure. While the conductor jacket is of constant cross section at all magnet locations, the outboard guard vacuum varies in size, being smaller near the minor radii (as shown in Figure 2) and larger near the major radii.

Cooldown and warmup gaseous helium enters the magnet at the bottom of each coil, as does liquid helium during steady state operation. All fluids exit at the highest location on each coil. Separate flow branches are incorporated for the conductor region and the guard vacuum, respectively, because the guard vacuum must be evacuated following cooldown. Gaseous (and liquid) helium flows uniformly through interstices in the liberally-ventilated conductor windings and interlayer/interturn insulation.

3. THE THERMAL ANALYSIS MODEL

3.1 Nodal Arrangement. The basic node pattern employed in the detailed (large) analysis models is shown in Figure 3, in which correspondence of the thermal and structural analysis models is apparent. The Figure 3 section is typical of the arrangement in each of 11 groups, extending from the major radius of a single coil quarter section to its minor radius. Note the additional external stiffener nodes at the juncture of groups 1 through 8. Not shown in Figure 3 are the intercoil structure modeling details. The latter was accomplished by additional box-like node groups. The node density reflected in the Figure 3 section is an approximate minimum for adequately assessing transverse temperature differentials in the magnet structure.

The nodal arrangement shown in Figure 3 does not comprise an entire analysis model. Rather, it simply describes a recurring pattern employed variously in thermal models discussed in succeeding paragraphs. Moreover, it will be seen that definition of longitudinal structural temperature differentials and cooldown/warmup durations were best served by formulation of a small macro-model of the entire magnet (small only in terms of node quantity). The macro-model structural and flow nodes were each thermophysically equivalent to the sum of all corresponding structural and flow nodes of a single group, eleven of which are shown in Figure 3. Multiple parallel inter-node longitudinal resistances were also collapsed to form macro-model internode resistances.

It will be noted in comparing Figures 2 and 3 that each conductor node represents a region containing multiple turns of conductor. Accurate representation of conductor node effective thermophysical, thermodynamic, and transport properties necessitated prior computations based on the repeating pattern of conductor geometry shown in Figure 4. Results included conductor node (Figure 3) effective mass, cross-sectional flow area, convective heat transfer surface area, and temperature-dependent values of anisotropic conductivity and specific heat.

3.2 Thermal Model Basic Formulations. The Convair Thermal Analyzer computer program was employed in performing the analyses of this study. The Thermal Analyzer is a versatile, general-purpose heat conduction procedure, programmed in FORTRAN IV for the Control Data Corporation (CDC) CYBER 70 series computer. It is capable of either explicit or implicit solution of node temperature values. It contains a broad range of built-in analytical correlations, permitting convenient numerical simulation of relatively massive applications, as represented by the MFTF magnet cooldown and warmup analyses. A brief description of the thermal analyzer modeling correlations employed in the analyses will serve to clarify discussion of the thermal models.

Figure 5 summarizes the basic analytical devices employed throughout the simulations. The five block-type nodes, elemental lumped-parameter rectangular parallelepipeds of dimensions x, y, and z, are characteristic of the structure nodes of Figure 3. Zero-mass, interface nodes can be employed at the juncture, or on the surface of block nodes. Figure 5 resistances R_{b1} and R_{b2} show the formulation of block-to-block and block-to-interface linkages, respectively. Flow nodes, linked in the flow direction by psuedo-resistances, R_f, honor the quasi-steady flow equation presented in Figure 5. The latter feature is accommodated by a complex numerical formulation which is fundamentally different from the conduction equation. Its development exceeds the scope of this paper. Flow nodes are linked to surface nodes by convective resistances, R_h, which are internally formulated and continuously re-evaluated on the basis of temperature-dependent thermo-physical fluid properties contained in Thermal Analyzer permanent storage. Steady flow simulations can be directed to multiple parallel branches, as shown in Figure 6, and can be subsequently merged as the particular application might demand.

3.3 Helium Flow Distribution and Schedules. The MFTF magnet cooldown and warmup through-flow was modeled in terms of two basic flow sources (supplying the conductor and the guard vacuum), each of which was branched to parallel successions of flow nodes. Local flow rates contacting each convectively cooled or heated node were apportioned based on ratios of local to total cross-sectional flow area. Conductor node convective linkages were based on a laminar flow Nusselt number of 4.0, an effective hydraulic diameter of 0.131 cm, and a surface area per conductor of 8.17 cm^2/cm (each conductor node contains 348 turns). Guard vacuum flow passages of 0.95 cm nominal depth cover 50% of the case inner surface, and a Nusselt number of 4.0 was again assumed.

A range of helium total flow rates and supply temperature schedules was investigated, as shown in Table I. Preliminary analyses assumed supply temperature to be controlled on the basis of a measured case temperature at the upstream minor radius of one coil, noted in Table I as T_s. As will be seen, longitudinal temperature gradients subsequently dictated employment of a stepwise schedule of supply temperature management, also shown in Table I.

Guard vacuum cooldown and warmup helium flow enter and pass through the coil extension structure prior to entering the guard vacuum, and approximately 60% of the latter flow is diverted through the intercoil structure. Because the coil extension and intercoil structures do not contain baffles for efficient convective scrubbing of the surfaces, the interior of the structures comprises a series of relatively large plenums. Convective heat transfer at the plenum surfaces was therefore computed (continuously, a program subroutine) on the basis of a turbulent flow Grashof-Prandtl correlation:

$$Nu = 0.13\,(GrPr)^{2/3}. \qquad (1)$$

3.4 Preliminary and Interim Analysis Models. Employing appropriate combinations of the foregoing methods, the cooldown and warmup analysis numerical model was initially formulated to model the magnet assembly in its prior orientation, with vertical alignment of the z-axis. The latter orientation permitted realistic thermal simulation by means of a quarter-symmetric model containing 738 nodes (Figure 7). Because helium entered and exited the magnet at the major and minor radii as shown in Figure 7, a single 738-node model could be employed to analyze the complete magnet assembly, requiring only simple redirection of the helium flow nodes.

Reorientation of the magnet assembly necessitated relocation of the helium entry and exit ports, and eliminated the convenient thermal symmetry of the original orientation. It therefore became necessary to modify the cooldown and warmup analysis model to the Figure 7 interim configuration, in which two analysis models were required to assess the transverse temperature differentials in the thermally-asymmetric assembly. The Figure 7 interim models, containing 629 nodes and 1,280 nodes, respectively, required complicated imposition of boundary condition and initial condition temperatures, as well as a significantly increased run time on the MNFECC computer system due to the sheer size of the model.

3.5 Final Configuration of the Analysis Model. Following an increase in the number of case-stiffening structural members, and to permit execution of multiple cooldown runs over a range of flow rates, two major modifications were incorporated in the modeling scheme. The 1,280-node model of Figure 7 was resolved into two separate models, shown in Figure 8 as "Large Model 1" and "Large Model 2." Also, as previously noted, the detailed node-resistor arrays of the large models were analytically collapsed into equivalent mass nodes and flow nodes. The entire magnet was thus modeled with 44 mass nodes. The so-called "Small Model" (Figure 9) permitted economical execution of repeated runs to assess cooldown/warmup sensitivity to flow rate and supply temperature. It also yielded boundary condition temperatures for imposition in the large model studies. The analysis models and their respective functions can thus be summarized as follows:

Analysis Model	Analysis Data
Large Models 1 and 2	Transverse Gradients
Small Model	Longitudinal Gradients
Small Model	Cooldown/Warmup Time

4. THERMAL RESPONSE DATA

4.1 Data Overview. Execution of repeated large model and small model computer runs covering the Table I flow schedules yielded a massive quantity of analysis data. Of particular interest to this paper are pertinent trends and correlations of resulting structural temperature differentials and cooldown/warmup durations. Data presentation will therefore be limited to representative temperature excursion plots which, together, demonstrate pertinent trends. The data include large and small model thermal response to the maximum flow rate of Table I cooldown schedule (1), and to the final recommended 100 g/s flow rates with Table I cooldown and warmup schedules (2).

4.2 Large Model Analysis Data. As expected, the most severe transverse case temperature gradients were induced as a result of the external stiffeners, which do not have the benefit of direct convective heat transfer. This effect is typified in the large model temperature distribution transients of Figure 10, in which the data corresponds to the Figure 3 node group number 6 location. The external stiffener is seen to lag the remaining structure during cooldown, and the effect is clearly intensified with increasing flow rate.

4.3 Small Model Analysis Data. Figure 11 shows the longitudinal temperature profiles at successive intervals during cooldown with flow schedules (1) and (2) of Table I. The severe longitudinal differentials caused by cooldown schedule (1) were found to be essentially independent of flow rate, but were strongly affected by the schedule of helium supply temperature management. The latter effect dictated adoption of cooldown schedule (2), in which a stepwise decreasing supply temperature is employed. Warmup temperature profiles for a constant 100 g/s flow rate and the Table I warmup (2) supply temperature schedule are shown in Figure 12.

5. TEMPERATURE DIFFERENTIALS AND COOLDOWN DURATIONS

Cooldown duration and corresponding transverse and longitudinal case temperature differentials are summarized in Figure 13 as functions of cooldown flowrates. Maximum allowable stresses induced by transverse temperature differentials were encountered with cooldown schedule (1) and 180 g/s flow at 300K return temperature. The resulting cooldown duration of only 29 hr (Figure 13) was deemed unnecessarily rapid. Moreover, resulting stresses induced by longitudinal gradients proved to be excessive, necessitating stepwise supply temperature management, as noted above. Table I cooldown schedule (2) with 100 g/s total flow rate was therefore recommended to ensure comfortable levels of thermally-induced stresses, with an acceptable cooldown duration of 82 hr.

Longitudional temperature differentials for total flow rates of 85 g/s and 119 g/s were imposed on separate legs of a single magnet to evaluate thermally-induced stresses resulting from such a cooldown flow asymmetry. The latter condition represents a severe imbalance, in which helium mass flow in one leg would be 40% greater than that of the other leg. Resulting stresses proved to be mild. It was therefore concluded that a nominal cooldown flow rate of 100 g/s with the stepwise supply temperature management of Table I would yield a cooldown duration of 82 ± 10 hr, and that a severe flow asymmetry of 19 g/s and 21 g/s in opposing legs of a single magnet [(29 + 21) × 2 = 100] would not yield unacceptable stresses.

It may be noted that warmup of the magnet with the Table I schedule (2) supply temperatures and 100 g/s total flow is markedly slower than the corresponding cooldown, and total warmup duration is 142 hr. The latter effect is apparently related to the high heat capacity of the magnet at later stages of warmup, coupled with simultaneously reduced convective heating temperature potential. The flow asymmetry logic of the preceding paragraph would have similar application to a warmup situation.

6. CONCLUSIONS

1. Detailed thermal analyses of the MFTF superconducting magnet have been conducted. The analyses have yielded a broad range of magnet cooldown and warmup transient thermal response data, permitting successful definition of preferred cooldown and warmup operating procedures, consistent with acceptable levels of thermally-induced stresses.

2. The MFTF magnet structural configuration has been detailed in this paper. The physical and thermodynamic mechanism of cooldown and warmup by means of helium throughflow has been described and quantified.

3. Thermal-analytical modeling methods have been presented as they were employed in the analyses, including computer simulation correlations. The analysis models are representative of the level of detail required to support structural analyses of large magnet structures.

4. Cooldown analyses employing the Figure 8 (large) model have yielded detailed temperature excursion and transverse temperature differential data. Transverse thermal stresses are acceptable to a maximum flow rate of 180 g/s. However, limiting thermal stresses are caused by longitudinal temperature differentials obtained in analyses employing the Figure 9 (small) thermal model. The latter analyses show that cooldown of the magnet to 4.5K can easily be achieved within the 3- to 5-day goal cited by LLL. A gradually-decreasing or stepwise-decreasing helium supply temperature schedule must be employed to avoid excessive thermal stresses.

5. A total flow rate of 100 g/s, and the following supply temperature management schedule, are recommended for cooldown and warmup of the MFTF magnet system.

Cooldown/Warmup Time (hr)	Cooldown Helium Supply Temperature (K)	Warmup Helium Supply Temperature (K)
0 to 18	225	75
18 to 36	150	150
36 to 54	75	225
54	4.5	300

6. Predicted cooldown duration for 100 g/s total flow at the above supply temperature schedule is 82 ± 10 hr. Predicted warmup duration of 100 g/s total flow at the above temperature schedule is 142 ± 15 hr.

7. Severe flow rate asymmetry in opposing legs of a single magnet (nominal plus 16% versus nominal minus 16%) will not pose a thermal stress problem, but will only yield cooldown/warmup time dispersions in the respective legs.

Table I. MFTF magnet cooldown and warmup analysis flow rates and supply temperatures.

Flow Condition	Total Helium Flow Rate	Supply Temperature
Cooldown (1)	150 to 340 g/s at 300K*HRT	80K at †T_s 100K
	150 g/s at 4.5K to 100K HRT	4.5K at T_s 100K
Cooldown (2)	51 to 119 g/s, constant	225K, 0 to 18 hr
		150K, 18 to 36 hr
		75K, 36 to 54 hr
		4.5K 54 hr
Warmup (1)	136 to 340 g/s, constant	300K, constant
Warmup (2)	51 to 119 g/s, constant	75K, 0 to 18 hr
		150K, 18 to 36 hr
		225K, 36 to 54 hr
		300K 54 hr

* Helium return temperature.

† Control sensor temperature.

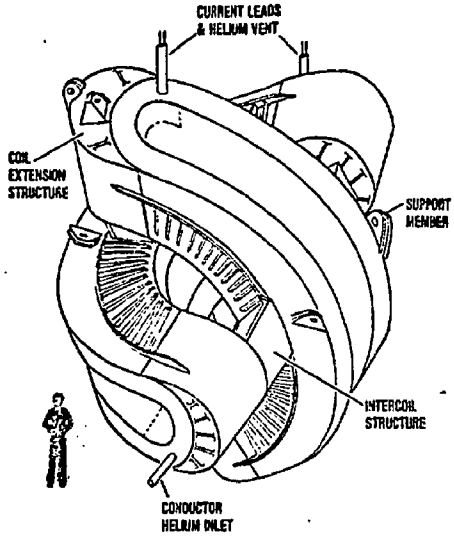
CURRENT LEADS
& HELIUM VENT
COIL
EXTENSION
STRUCTURE
SUPPORT
MEMBER
INTERCOIL
STRUCTURE
CONDUCTOR
HELIUM INLET

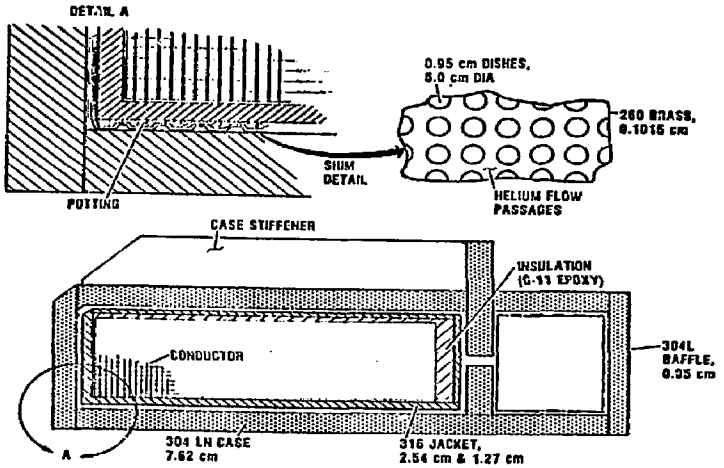
DETAIL A
POTTING
SHIM DETAIL
0.95 cm DISHES, 8.0 cm DIA
260 BRASS, 0.1016 cm
HELIUM FLOW PASSAGES
CASE STIFFENER
INSULATION (G-11 EPOXY)
CONDUCTOR
304L BAFFLE, 0.95 cm
A
304 LN CASE 7.62 cm
316 JACKET, 2.54 cm & 1.27 cm

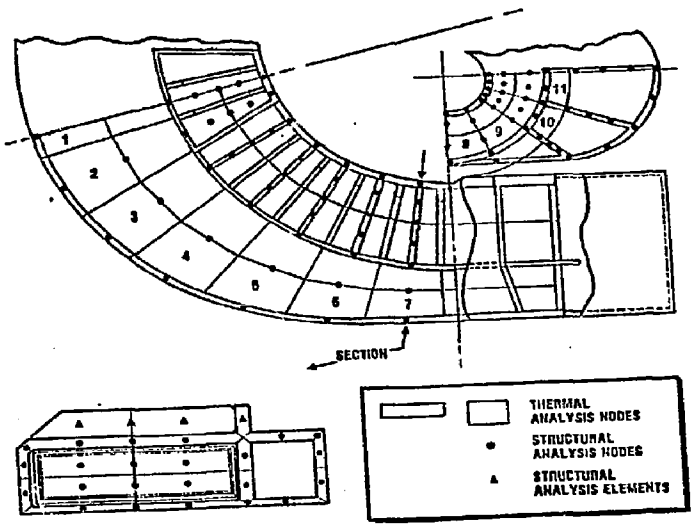
1
2
3
4
5
6
7
8
9
10
11
SECTION
THERMAL ANALYSIS NODES
STRUCTURAL ANALYSIS NODES
STRUCTURAL ANALYSIS ELEMENTS

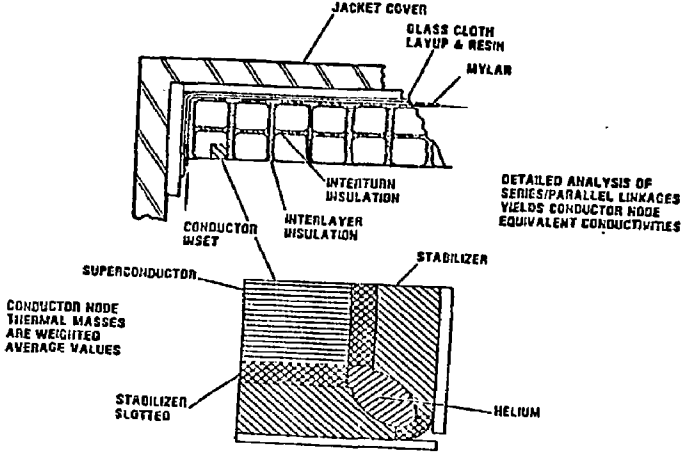
JACKET COVER
GLASS CLOTH LAYUP & RESIN
MYLAR
INTERTURN INSULATION
CONDUCTOR INSET
INTERLAYER INSULATION
DETAILED ANALYSIS OF SERIES/PARALLEL LINKAGES YIELDS CONDUCTOR NODE EQUIVALENT CONDUCTIVITIES
STABILIZER
SUPERCONDUCTOR
CONDUCTOR NODE THERMAL MASSES ARE WEIGHTED AVERAGE VALUES
STABILIZER SLOTTED
HELIUM

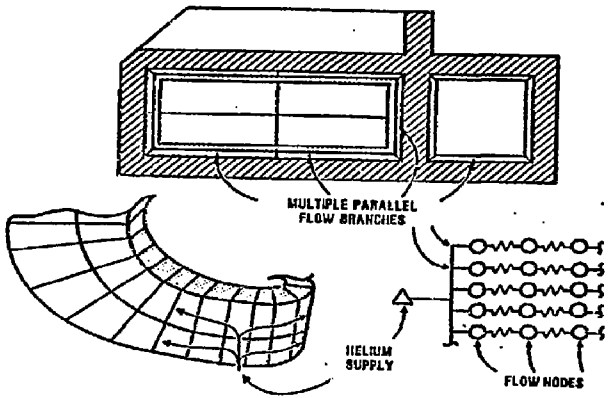
MULTIPLE PARALLEL
FLOW BRANCHES
HELIUM
SUPPLY
FLOW NODES

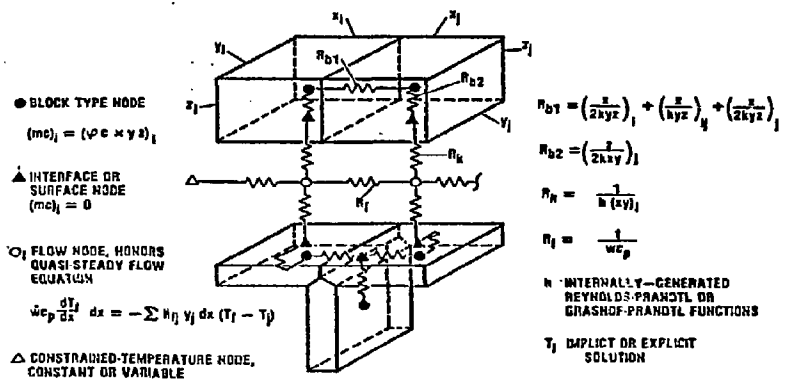
● BLOCK TYPE NODE
$(mc)_i = (\rho c \times y z)_i$
▲ INTERFACE OR SURFACE NODE
$(mc)_i = 0$
O_f FLOW NODE, HONORS QUASI-STEADY FLOW EQUATION
$\dot{w} c_p \frac{dT_f}{dx} dx = -\sum h_{fj} y_j dx (T_f - T_j)$
△ CONSTRAINED-TEMPERATURE NODE, CONSTANT OR VARIABLE
$R_{b1} = \left(\frac{x}{2kyz}\right)_i + \left(\frac{x}{kyz}\right)_j + \left(\frac{x}{2kyz}\right)_j$
$R_{b2} = \left(\frac{x}{2kxy}\right)_j$
$R_h = \frac{1}{h (xy)_i}$
$R_f = \frac{1}{\dot{w} c_p}$
h INTERNALLY-GENERATED REYNOLDS-PRANDTL OR GRASHOF-PRANDTL FUNCTIONS
T_j IMPLICIT OR EXPLICIT SOLUTION

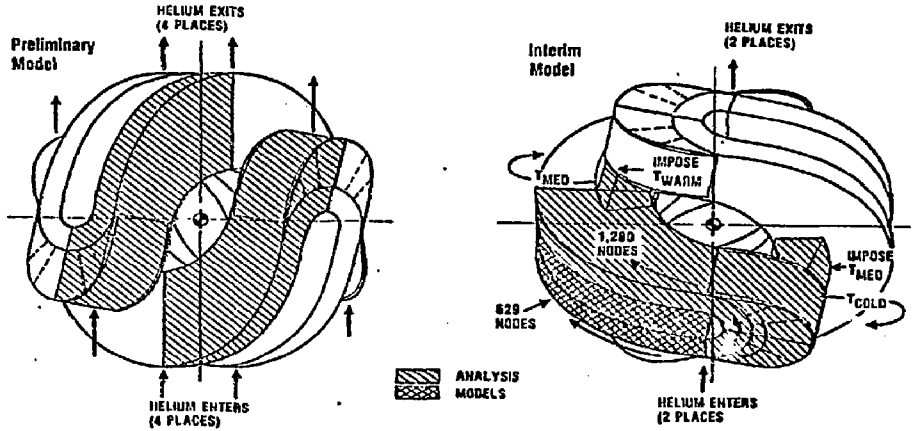
Preliminary Model
HELIUM EXITS (4 PLACES)
HELIUM ENTERS (4 PLACES)
Interim Model
HELIUM EXITS (2 PLACES)
HELIUM ENTERS (2 PLACES)
IMPOSE T_{WARM}
T_{MED}
1,280 NODES
629 NODES
IMPOSE T_{MED}
T_{COLD}
ANALYSIS MODELS

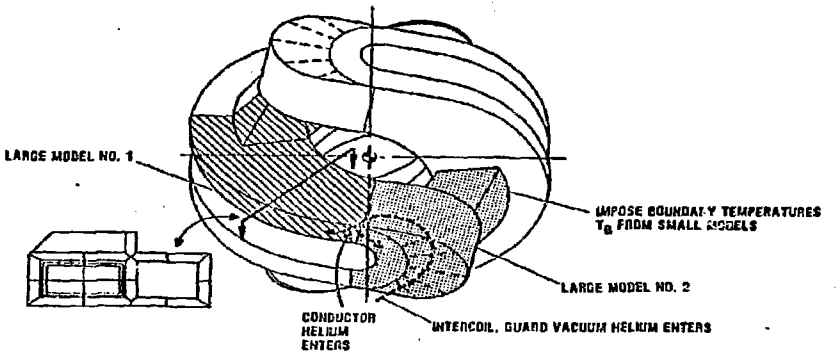

PLAN AS VIEWED FROM BELOW MAGNET

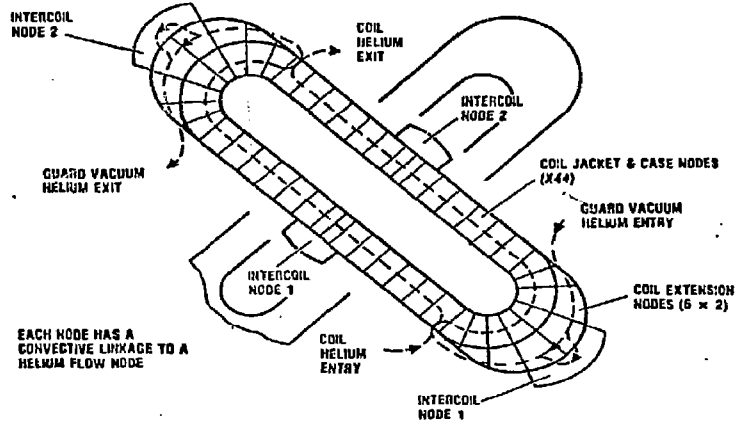
INTERCOIL NODE 2
COIL HELIUM EXIT
INTERCOIL NODE 2
GUARD VACUUM HELIUM EXIT
COIL JACKET & CASE NODES (X44)
GUARD VACUUM HELIUM ENTRY
INTERCOIL NODE 1
COIL EXTENSION NODES (6 x 2)
EACH NODE HAS A CONVECTIVE LINKAGE TO A HELIUM FLOW NODE
COIL HELIUM ENTRY
INTERCOIL NODE 1

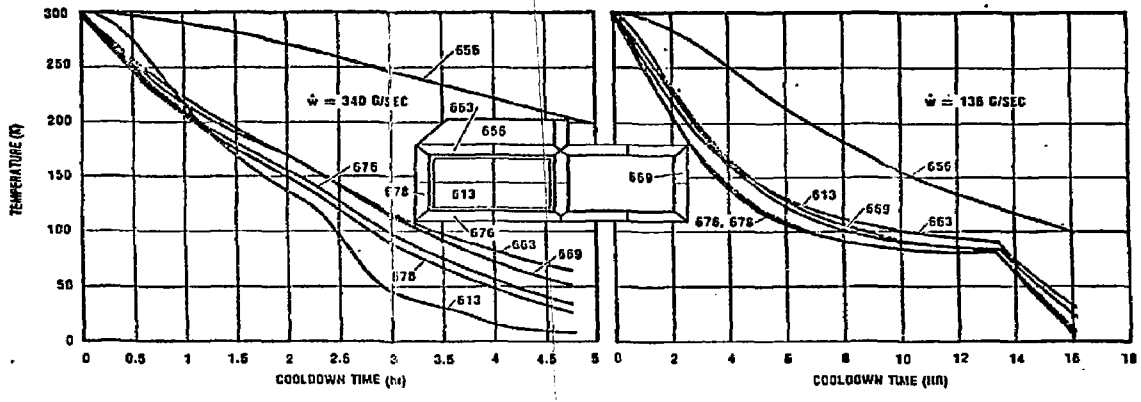
TEMPERATURE (K)
300
250
200
150
100
50
0
0
0.5
1
1.5
2
2.5
3
3.5
4
4.5
5
COOLDOWN TIME (hr)
$\dot{w}$ = 340 G/SEC
656
663
656
675
678
613
669
676
663
669
678
613
$\dot{w}$ = 136 G/SEC
656
613
669
663
676, 678
0
2
4
6
8
10
12
14
16
18
COOLDOWN TIME (hr)

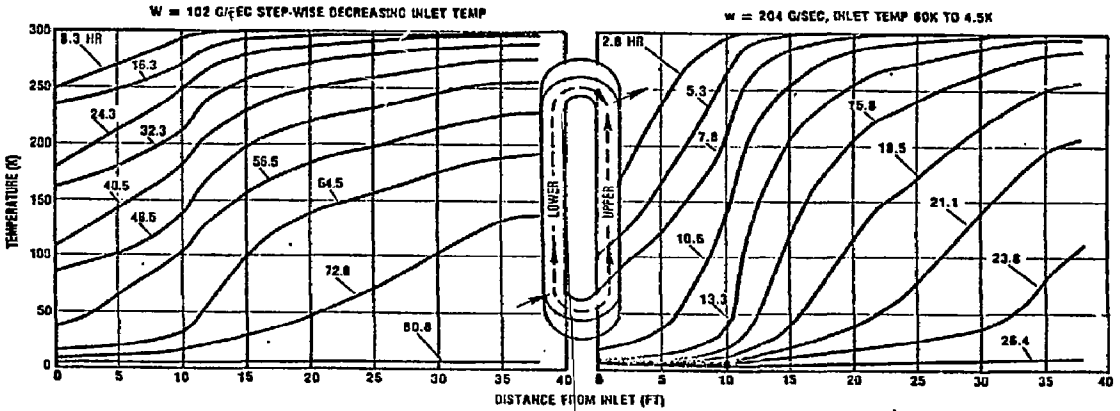
W = 102 G/SEC STEP-WISE DECREASING INLET TEMP
w = 204 G/SEC, INLET TEMP 60K TO 4.5K
8.3 HR
16.3
24.3
32.3
40.5
48.5
56.5
64.5
72.8
80.8
2.8 HR
5.3
7.8
10.5
13.3
15.8
18.5
21.1
23.8
26.4
LOWER
UPPER
TEMPERATURE (K)
DISTANCE FROM INLET (FT)
0
50
100
150
200
250
300
0
5
10
15
20
25
30
35
40

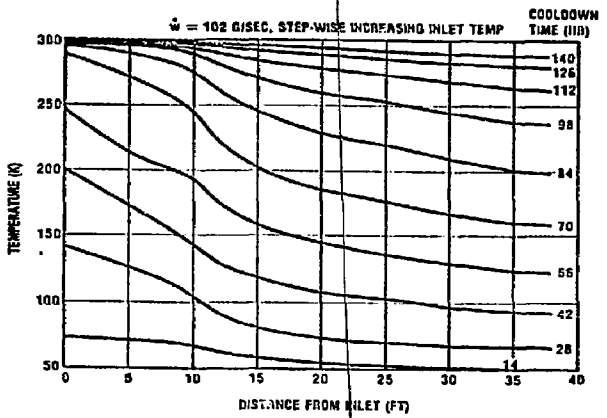
$\dot{w}$ = 102 G/SEC, STEP-WISE INCREASING INLET TEMP
COOLDOWN TIME (HR)
140
126
112
98
84
70
56
42
28
TEMPERATURE (K)
300
250
200
150
100
50
0
5
10
15
20
25
30
35
40
DISTANCE FROM INLET (FT)

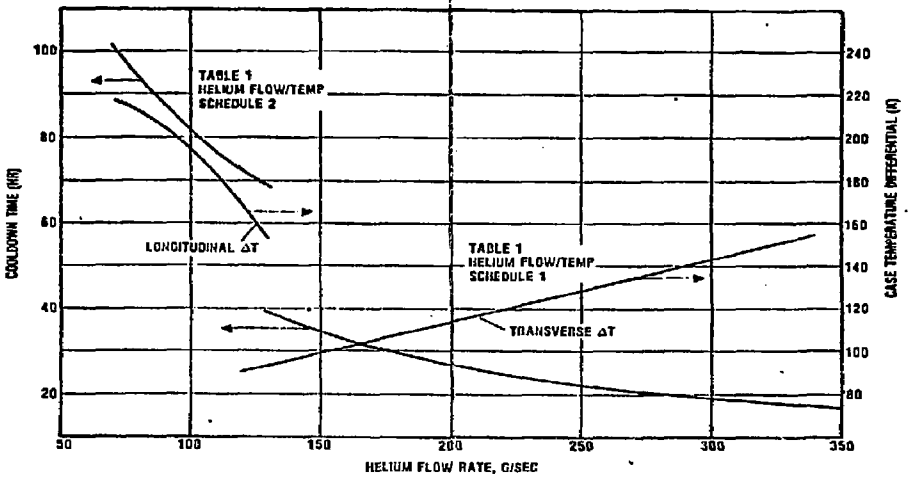
TABLE 1
HELIUM FLOW/TEMP
SCHEDULE 2
LONGITUDINAL ΔT
TABLE 1
HELIUM FLOW/TEMP
SCHEDULE 1
TRANSVERSE ΔT
COOLDOWN TIME (HR)
CASE TEMPERATURE DIFFERENTIAL (K)
HELIUM FLOW RATE, G/SEC
100
80
60
40
20
240
220
200
180
160
140
120
100
80
50
100
150
200
250
300
350

NOTICE